Global changes in floods and possible mechanisms

Shuyun Feng[1], Jianyu Liu[1], Yongqiang Zhang[2], Hylke E Beck[3], Xihui Gu[4,5]

[1]Laboratory of Critical Zone Evolution, School of Geography and Information Engineering, China University of Geosciences, Wuhan 430074, China

[2]Key Lab of Water Cycle and Related Land Surface Processes, Institute of Geographic Sciences and Natural Resources Research, Chinese Academy of Sciences, Beijing 100101, China

[3]Department of Civil and Environmental Engineering, Princeton University, Princeton, New Jersey, USA

[4]State Key Laboratory of Simulation and Regulation of Water Cycle in River Basin, China Institute of Water Resources and Hydropower Research

[5]Department of Atmospheric Science, School of Environmental Studies, China University of Geosciences, Wuhan 430074, China

Corresponding author: Jianyu Liu (liujy@cug.edu.cn); Xihui Gu (guxihui421@163.com)

Key Points:

- We perform a global assessment of trends in multidimensional flood behaviors (magnitude, frequency, and duration)
- Global floods have become not larger but more frequent
- Dams have the larger impacts on the flood magnitude, followed by flood frequency and duration

Abstract

While warming temperatures are known to increase atmospheric moisture capacity and heavy precipitation frequency; as yet there is little evidence for corresponding increases in floods. This study comprehensively examines global changes in multidimensional flood behaviors (magnitude, frequency, and duration), and aims to identify the possible mechanisms behind the heavy precipitation and flood change dichotomy. Our global assessment shows that floods become more frequent but not larger. Regionally, consistent changes can be observed among multidimensional flood behaviors, i.e., floods becoming larger in magnitude, more frequent, and longer in duration in some regions (e.g., North Europe), while smaller, less frequent, and shorter in other regions (e.g., South Australia). Attribution analysis indicates that spatial patterns of global flood trends are primarily controlled by shifts in atmospheric circulation patterns, terrestrial water storage changes and temperature increases. The dams are crucial for reducing the floods, with the greatest impacts on flood magnitude, followed by flood frequency and duration. Catchment characteristics (i.e., vegetation coverage, irrigation, and urbanization) regulate the response of flood changes to changing environments.

Plain Language Summary

The global warming is expected to intensify hydrological cycle and makes the precipitation and extreme events increasing. This can often deceive people into thinking that floods and hence risk are raising. However, our knowledge about the global changes in multidimensional floods (i.e., magnitude, frequency, and duration) is still limited, restricted by spatial coverage and number of hydrological stations. Here we assessed the changes in multidimensional of floods at both global and regional scales during 1960-2017, based on combined dataset including more than 20,000 gauging stations worldwide. Our results indicate that global floods increase more

widespread in frequency, but not the flood magnitude and duration. Then, we further investigate the reasons why the increased heave precipitation does not lead to corresponding increases in floods. Our findings shed new light on global multidimensional flood changes, which have important implications for climate change impact assessments and flood managements.

1 Introduction

Flooding is one of the most devastating natural disasters worldwide, resulting more than half of a million deaths over the past thirty years (CRED, 2015; Doocy et al., 2013; Lee et al., 2018). Any changes in river floods would have significant impacts on the design of flood protection measures and flood risk assessment (Bloschl et al., 2019) Thus, it is crucial to examine how river floods have changed over time (Mallakpourand Villarini, 2015).

Although numerous progresses have been investigated in river flood changes over different regions, such as North America (Archfield et al., 2016; Hodgkins et al., 2019; Mallakpourand Villarini, 2015; Musselman et al., 2018; Slaterand Villarini, 2016), Europe (Hannaford et al., 2013; Hodgkins et al., 2017), Australia (Liuand Zhang, 2017; Liu et al., 2018) and Asia (Delgado et al., 2010), there is still very limited knowledge about global flood changes. As previous regional studies often used different strategies to select stations, it is difficult to draw a solid conclusion regarding global pattern in flood changes. Furthermore, flood changes vary not only by regions but also by flood dimensions, e.g., flood magnitude, frequency, and duration. However, in the limited global assessments of river flood changes (Do et al., 2017; Milly et al., 2002), only the peak-flow sampling technique (PF) has been adopted to extract flood magnitudes. It should note that there are some limitations by using PF alone: (1) only the changes in flood magnitude can be assessed; and (2) PF fixedly selects one flood event per year,

even though multiple floods may occur within a single year (Liu et al., 2017). The peaks-over-threshold sampling technique (POT), which identifies flood events using an optimized threshold value, allows us to obtain multiple floods within one year and extract the frequency and duration of floods (Archfield et al., 2016). Previously, based on the simulated runoff from satellite microwave and Water Balance Model outputs, Najibi and Devineni (2018) made a global assessment on flood frequency and duration. However, as stated by Najibi and Devineni (2018), there is a certain level of epistemic uncertainty in their results, limited by the imprecision in the estimation of floods from remote-sensing and model outputs. To our knowledge, no previous study has examined the global trends in multidimensional river floods (i.e., magnitude, frequency, and duration) based on the observed streamflow data from gauging stations. Moreover, few studies have addressed the possible causes behind flood changes across large spatial scale.

Based on the Clausius-Clapeyron relationship, global warming will enhance the moisture holding ability of the atmosphere (Sillmann et al., 2013). As a result, increases in heavy precipitation were observed in many regions around the globe (Asadiehand Krakauer, 2015). However, several studies shown that there was little evidence of increases in floods, and most results indicated that decreases in flood events were more prevalent than increases in many regions (Archfield et al., 2016; Do et al., 2017; Mallakpourand Villarini, 2015; Sharma et al., 2018). Therefore, there is an urgent need to understand why the increases in extreme precipitation have not resulted in flood increases.

Flood changes may be caused by multiple climatological, meteorological, anthropogenic, and hydrological factors *(Sharma et al., 2018)*. It has been suggested that rising temperatures intensify the soil moisture drying (Gu et al., 2019a; Gu et al., 2019b) and reduce terrestrial water

storage (i.e., groundwater, lakes, and reservoirs) (Slaterand Villarini, 2016), which may lessen the antecedent soil moisture and in turn may decrease flood magnitude, frequency, and/or duration. Furthermore, variations in atmospheric circulation can lead to storm mechanism changes as well as changes in catchment wetness states (Lu et al., 2013; Wasko et al., 2015). In addition, large-scale anthropogenic activities, such as dams construction (Mallakpourand Villarini, 2015), have greatly impacted the hydrological cycle, which may even surpass climate change impacts in some regions (Sharma et al., 2018). In addition to the abovementioned factors, floods are also influenced by catchment characteristics, such as vegetation coverage, irrigation, and urbanization (Hettiarachchi et al., 2018; Johnson et al., 2016). Although these factors have been individually known to contribution to regional hydrological changes across different regions, their impacts on global flood changes remain largely obscure. Hence, Sharma et al. (2018) suggested that future studies should focus on the relationship of flood changes to a series of factors.

Therefore, the main objectives of this study are to (1) examine the changes in multidimensional flood behaviors across the globe and (2) investigate the causes of global flood changes. Consequently, this study performs a global assessment of flood changes in the recent half century, considering multidimensional flood behaviors in magnitude, frequency and duration and using an integrated dataset with streamflow observations from more than 20,000 gauging stations worldwide (Figure 1).

2 Data

2.1 Hydrological data

The selection of abundant high-quality streamflow data is crucial for the detection of hydrological changes (Shengand Wang, 2012). However, limited by the number of hydrological

data, most studies concerning flood changes are restricted to regional or national scales. Here, we synthesized a global dataset consisting of 21,955 gauging stations with daily streamflow data (Figure 1), which was compiled from the following eight national and international sources:

(1). 9180 stations from the National Water Information System of the US (https://waterdata.usgs.gov/nwis) and GAGES-II database (Falcone et al., 2010).

(2). 4628 stations from the Global Runoff Data Centre (GRDC; http://grdc.bafg.de).

(3). 3029 stations from the HidroWeb portal of the Brazilian Agência Nacional de Águas (http://www.snirh.gov.br/hidroweb).

(4). 2260 stations from EURO-FRIEND-Water (http://ne-friend.bafg.de).

(5). 1479 stations from the Canada National Water Data Archive (HYDAT; https://www.canada.ca/en/environment-climate-change).

(6). 776 stations from the Commonwealth Scientific and Industrial Research Organization (CSIRO) and Australian Bureau of Meteorology (http://www.bom.gov.au/waterdata) (Zhang et al., 2013).

(7). 531 stations from the Chilean Center for Climate and Resilience Research (http://www.cr2.cl/recursos-y-publicaciones/bases-de-datos/datos-de-caudales) and CAMELS-CL (Alvarez-Garreton et al., 2018).

This streamflow dataset was initially filtered using the following four steps: (1) the stations with more than 15% missing daily observations were discarded; (2) the years with missing daily observations were deleted for each station; (3) the stations with record ended before 2000 were exclude; and (4) the stations with less than 30 years during 1960-2017 were generally exclude. To make the spatial distribution of stations more even across the globe, in the continent with the highest station densities, i.e., North America, only the stations with at least 50-year records were

considered; while in the continent with the low station densities, i.e., Asia and Arica, the stations with more than 25 years of data were considered. In China, the stations with more than 18-year records were considered, since most stations in China just have 18-year records. As a result, there are 6573 stations meeting the requirement, with mean record length of 50 years during 1960-2017.

2.2 Meteorological data and catchment characteristics

Extreme precipitation, temperature, and catchment characteristics for each catchment were extracted to assess their impacts on flood changes. The daily precipitation dataset with 0.1 degrees was obtained from Beck et al. (2019). The monthly temperature data were obtained from the Princeton Global Forcing (PGF) dataset (http://hydrology.princeton.edu/data.pgf.php). The following catchment characteristics were used for the causality analysis: irrigated fraction, land cover, normalized difference vegetation index (NDVI), population, reservoir capacity, topographic slope, surface elevation, and soil texture. See Table 1 for data source details. It's worth to mention that the meteorological data and catchment characteristics for each catchment are the mean value over the entire contributing area, which were extracted by using the shapefiles of catchment boundary.

In addition, the Dams were taken from the Global Reservoir and Dams (GRanD) dataset (http://globaldamwatch.org/data/#core_global). GRanD dataset includes 8,502 large dams with a capacity of larger than 0.1 km^2, which includes 1480 dams designed for flood control. Although this dataset was integrated from various research institutes, it is hard to include overall dams across the globe. The number of dams (only these designed for flood control was considered) in each catchment was identified based on the shapefiles of catchment boundary. If there is one (or

more) flood-control dam within the catchment boundary of a hydrological station, then we considered it as a dam-affected station.

2.3 GRACE data

The Gravity Recovery and Climate Experiment (GRACE) satellite pair provides global monthly terrestrial water storage change (TWSC) data, which has been deemed valuable for a wide variety of applications, such as groundwater monitoring (Niu et al., 2014), flood forecasting (Reager et al., 2014), and drought monitoring (Long et al., 2014). The GRACE data are expressed in centimeters of equivalent water thickness with a spatial resolution of 0.5° and have been available since 2002. Although the temporal coverage of GRACE is relatively limited, these data may provide valuable information for hydrological simulations and predictions (Slaterand Villarini, 2016). The GRACE dataset was processed by the Jet Propulsion Laboratory with improved signal recovery, which can be downloaded from the GRACE Tellus website (https://grace.jpl.nasa.gov/data/get-data/). The relationship of TWSC to flood changes was assessed by using the common coverage periods of TWSC and floods, that is, during 2001-2015.

2.4 Atmospheric circulation data

To analyze the potential effects of atmospheric circulation on flood changes, we obtained the complete meteorological reanalysis dataset from the National Centers for Environmental Prediction and the National Centre for Atmospheric Research (NCEP/NCAR) (Kalnay et al., 1996). The NCEP/NCAR reanalysis dataset has been widely used in the global atmospheric circulation study, and this dataset was created through data assimilation with a state-of-the-art analysis/forecast system (Kalnay et al., 1996) and continually updated globally since 1948. We selected monthly horizontal wind and geopotential height at 850 hPa with a spatial resolution of

2.5°×2.5°, which is available at the NCEP/NCAR website (https://www.esrl.noaa.gov/psd/data/gridded/data.ncep.reanalysis.pressure.html).

3 Methods

3.1 Flood sampling

We applied both PF and POT sampling to get the series of flood magnitude, frequency and duration based on the observed daily streamflow data. The PF sampling extract seasonal and annual flood magnitude with maximum values of streamflow. The POT sampling obtained flood frequency and duration by accounting flood events over a threshold, which helps to capture a wide of flood events that are not constrained by the time when floods occurred. By using several flood series extracted by different flood thresholds (with averages of 3, 2, 1 and 0.5 flood events per year), Liu and Zhang (2017) found that the flood thresholds have limited impacts on the results of flood changes. To extract enough flood events and avoid counting the same events twice, following the study of Mallakpour and Villarini (2016), we used an average of 2 floods events per year and a two-week time window to ascertain the flood thresholds for each station. Then, to obtain the seasonal flood frequency and duration, the flood events during each year were separated into different seasons, i.e., spring (March to May), summer (June to August), autumn (September to November), and winter (December to February).

3.2 Trend analysis

The Mann-Kendall test was used to examine the trend significant of floods at 95% confidence level (Hirschand Archfield, 2015). To investigate whether the percentage of stations showing significantly increase/decrease was significant, Mann-Kendall test combining with the bootstrap sampling were applied (Do et al., 2017; Ishak et al., 2013; Westra et al., 2013). The steps in this approach are as follows:

1. Resample with a replacement time series of floods to set up a new dataset with the same length but different year order;

2. Apply the Mann-Kendall test to examine the resampled flood at 95% confidence level, and count the percentage of stations showing significant trend in increase and decrease;

3. Repeat 2000 times for the above two steps to obtain the percentage distribution of stations with significant trend;

4. Calculate the 95^{th} percentile of percentage distribution, which represents the percentage of stations showing significant trend by random chance at 95% confidence level.

The percentage of significant trends assessed by observed datasets were compared to the 95^{th} percentile of percentage distribution assessed by resampled datasets. The null hypothesis is rejected when the former larger than the later, implying the observed percentage is not simply due to random, but significant at 95% confidence interval (Do et al., 2017). In addition, a moving-blocks bootstrap was to applied to avoid the intra-block correlation among different stations (Kiktev et al., 2003).

The flood trends were also assessed at the regional scale for the 17 subcontinents (Fig S1). The subcontinents were divided in the IPCC 5^{th} Assessment Report (http://www.ipcc-data.org/guidelines/pages/ar5_regions.html), which were widely applied to regional and global studies (Gudmundsson et al., 2019; Lehmann et al., 2018). The regional trends were calculated by the mean magnitude of trends ($\bar{T}$) with consideration of all stations on each subcontinent. In addition, regional Mann-Kendall test (rkt) was applied to investigate the confidence level of regional trend for each subcontinent (Henseland Frans, 2006). To avoid the intra-block correlation among different stations, the correction for the correlation among blocks was used (Hirschand Slack, 1984). The significantly regional trend was identified when the two-sided p-

value (after correction for the intra-block correlation) small than 0.05. The regional trend test was carried by using the freely available *rkt* in *R* language (Marchetto et al., 2013).

4 Results

4.1 Global pattern of flood trends

A global assessment shows that multidimensional floods (magnitude, frequency, and duration) do not change uniformly and vary over different regions (Figure 2). Clustering of increasing trend in multidimensional floods can be observed over western Europe, northern Australia, northeastern coastal of North America, and southern Brazil, while decreasing trends are sporadically distributed in western North America, eastern Brazil, North China, and southern Australia.

For flood magnitude, more stations show significantly decreasing trend (SDT) than significantly increasing trends (SIT), with the percentage of 10.1% for the former and 7.1% for the later. On the contrary, for flood frequency, there are more station with SIT than that with SDT, with 565 (8.6%) stations for the former, but 473 (7.2%) for the later. For flood duration, there is no obvious difference in the percentage of station showing SDT and SIT. By investing the flood changes across the central United States, Mallakpour and Villarini (2015) found that limited evidence of significant changes in flood magnitude, while strong evidence pointing to an and increasing flood frequency. Furthermore, Hirsch and Archfield (2015) concluded that global flood not higher but more often across the central United states. This finding is also true for the global flood changes (Figure 2 a-b).

Owing to randomness, there will be a certain percentage of stations showing significant trends (Archfield et al., 2016). Therefore, we applied a moving blocks bootstrap to test the field significance of the percentages of stations showing significant trend. Figure 3 shows that all the

percentages reject the null hypothesis of no changes in floods, implying the percentages are not caused by random changes and are significant at 95% confidence level.

In most cases, the signs of regional flood trends are consistent in different flood dimensions (Figure 4). Consistent increasing regional trends in multidimensional floods are observed in Amazon, Central Europe, Canada/Greenland/Iceland, Central North America, East North America, North Europe and Southeastern South America. In contrast, consistent decreasing trends are detected in Alaska/N.W. Canada, North Australia, North-East Brazil, South Australia/New Zealand, West North America. These results are broadly consistent with the previous studies in different regions, such as Europe (Bloschl et al., 2019; Gudmundsson et al., 2017; Stahl et al., 2012), America (Mallakpourand Villarini, 2015), Amazon (Marengo et al., 1998), Southern Africa (Fanta et al., 2001), Australia (Ishak et al., 2013; Liuand Zhang, 2017).

As for the mean changes in multidimensional floods during 1960-2017, regional trends range from an increase of 6.6% to a decrease of -16.7% per decade (Figure 4). In the regions with significant trends, the percentages of stations showing significant trend and the mean Sen-Theil slope are generally larger than the global average. These results imply that the regional trend can represent the general regional changes of flood to some extent. The strongest signal is observed in South Australia/New Zealand, where the regional trends of flood magnitude, frequency, and duration decrease by more than 9.5% per decade, and more than 19.5% of stations showing SDT (Table 2). In contrast, the regional trends of flood magnitude and duration in North Europe are significantly increasing, with more than 15% stations showing SID. These results indicate that flood magnitude is generally connected to flood frequency and duration, implying that the floods tend to be larger and more frequent and last longer in some regions, while smaller, less frequent and shorter in other regions.

4.2 The impacts of climate conditions and TWSC on flood trends

Since the floods result from the interaction between climate conditions (e.g., heavy precipitation, temperature, and atmospheric circulation), TWSC and catchments characteristics, here we investigated the spatiotemporal changes of these drives and their relationship to flood trends.

Obviously, larger and more frequent heavy precipitation has been observed around the world (Figure 5a-b), which was also found by previous studies (Donat et al., 2016). However, this phenomenon is largely inconsistent with global patterns in flood changes. Although the floods are generally significantly correlated with heavy precipitation (Figure 6), many regions show inconsistent tends between heavy precipitation and floods. Overall, there are 45.0% catchments showing different changing direction in the trends between heavy precipitation and floods magnitude. For all the catchments (488) showing SIT in heavy precipitation, there are only 34 (7.0%) catchments showing SIT in flood magnitude, while 23 (4.7%) catchments showing SDT. Therefore, although the heavy precipitation is usually considered as an important factor of flood generation, the changes in heavy precipitation have limited impacts on flood changes. This finding is consistent with the case in United States (Berghuijs et al., 2016). By investigating the dominant flood generating mechanisms across the United States, Berghuijs et al. (2016) found that heavy precipitation poorly explained the changes in flood. As a result, flood changes are usually affected by multiple driving factors (Hall et al., 2014).

Besides, Figure 6d shows that higher temperatures tend to associate with decreasing floods in most catchments. There is enough evidence that warming temperatures lead to greater evapotranspiration and drier soils (Sheffieldand Wood, 2008), which reduces the antecedent soil

moisture prior to floods. As a result, significantly increasing temperatures (Figure 6d) can lead to decreased flooding in most catchments.

The changes in atmospheric circulation would transform the dominant mechanism of a storm (Lu et al., 2013) by changing the heavy precipitation frequency and antecedent soil moisture conditions (Mallakpourand Villarini, 2016), which may further result in flood changes (Liu et al., 2018). Here, we examine the trends in the horizontal wind and 850 hPa geopotential height during the 1960-2017 period to investigate the possible impacts of atmospheric circulation changes on floods (Figure 7 and S3).

As is well known, prevailing westerlies play a key role in controlling climatic changes in Europe. During spring and winter, which are the major flood seasons across Europe (Figure S4), northern Europe is covered by an anomalous low-pressure center (Figure 7a; 7c), while southern Europe and their adjacent waters are controlled by an anomalous high-pressure center. The intensive horizontal pressure gradient force enhances the prevailing westerlies and transports warmer and wetter moisture from the Atlantic to northern Europe (Figure 7b and 7d). In addition, the low-pressure center is also accompanied by an updraft, which promotes moisture convergence and triggers more moisture condensation (Najibi et al., 2019). As a result, significantly increasing trends in floods are detected in northern Europe. In contrast, southern Europe is covered by an anomalous high-pressure center, which drives weaker prevailing westerlies and goes against moisture transport, causing decreasing flood trends (Figure 2).

Australia is controlled by an abnormal northerly wind, which results in warm-wet wind from the Pacific that covers northern Australia, while dry-heat wind from the arid inland covers southern Australia. As a result, distinct north-south differences in the flood trends are detected across Australia (Figure 2, see also Liuand Zhang, 2017). A similar pattern is also observed in

Brazil. Eastern Brazil is controlled by the inland west wind, while southern Brazil is controlled by an east wind from the south Atlantic. This leads to decreasing floods in eastern Brazil and increasing floods in southern Brazil (Figure 2). The detected consistent spatiotemporal patterns regarding the relationships between variations in atmospheric circulation and flood trends confirm that the shifts in atmospheric circulation have a great influence on flood changes.

Liquid water equivalent thickness measured by GRACE can be regarded as a proxy for regional TWSC (Slaterand Villarini, 2016). Interestingly, the flood changes in magnitude, frequency, and duration are generally consistent with the trends in TWSC (Figure 8), especially for the seasonal scale (Figure 9). Significantly increasing trends in floods are observed in the middle part of North America, where regional water storage changes also show increasing trends. On the other hand, significantly decreasing trends in floods over the middle part of southern America, southern Brazil, northern China, and southern Africa are also in line with the trend in TWSC. These results indicate that water storage changes are an important driver of flood changes. It should be noted that, limited by the record length of GRACE satellite, here the GRACE and flood trends are based on the periods of 2013-2016. Nevertheless, the spatial pattern in the flood trends showing in Figure 8 is broadly similar to that observed during 1960-2017 (Figures 2).

4.3 The impacts of catchment characteristics on flood trends

To investigate the influence of dams on multidimensional flood changes, we summarized the percentages of stations showing significant trend among the stations include one or more dams that designed for flood control and completed /operational during 1960-2017. And then we applied the bootstrap approach to test the significant level of the percentages (Figure 10). In contrast to the case considering all stations (Figure 2), the percentages of dams-impacts stations

with SIT in both magnitude, frequency and duration of flood are obviously smaller, with the percentage of 5.1%, 5.5%, and 8.8%, respectively; while that showing SDT are much larger, with the percentage of 20.4%, 13.2% and 12.1% respectively. In addition, the percentages of stations showing SIT in both flood magnitude and frequency are not significant. However, the percentages of stations showing SDT are significant at 95 confidence level, which implies that the null hypothesis of no changes in flood is rejected and the percentages are not caused by random chance. Interestingly, the dams have different impacts on flood magnitude, frequency, and duration. For flood magnitude, the percentages of stations showing SDT are four times larger than that showing SIT. For flood frequency and duration, however, these ratios are greater than two times and smaller than two times, respectively. These results indicate that the flood-control dams are indeed important for reducing flood, with the greatest impacts on flood magnitude, followed by flood frequency and duration.

To investigate the impacts of other catchment characteristics on flood trends, in the following analyses, we mainly focus on flood changes in the catchments that exclude large dams. We stratify the stations with few dams' impact into three groups with an equal number of stations (i.e., third quantiles) based on the values of each characteristic (Figure 11, S5 and S6). Significantly decreasing trends in multidimensional floods are more likely to occur in large catchments (Figure 11b, S5b and S6b), where the TWSC and evapotranspiration play more important roles (Ivancicand Shaw, 2015), particularly under a globally warming climate. In addition, the detected coverage area of storm events showed generally decreasing trends, which will further intensify the decreasing trends in large catchments (Chang et al., 2016; Wasko et al., 2016). With the increase of elevation, the percentage of stations showing SIT (SDT) in multidimensional floods tends to decline (rise). Irrigation enhances evapotranspiration and

reduces runoff prior to flood generation (Payero et al., 2008). Consequently, the percentages of stations showing SDT in the regions with high irrigation fraction are larger than that with low irrigation fraction (Figure 11d). At high latitudes, the percentages of stations showing significant increase in multidimensional floods are all obviously larger than that at low latitudes (Figure 11e), which is supported by increasingly wet conditions in the high latitude, such as north Europe (Stahl et al., 2010; Stahl et al., 2012) and north Asia (Tananaev et al., 2016). In addition, global climate model also projected that the wetting condition at high latitudes will continue in the future (Greve et al., 2018). Urbanization not only changes catchment permeability and roughness (Sharma et al., 2018) but also modifies precipitation intensity (Gu et al., 2019c). As a result, the percentages of stations showing SIT rise with the increase of urbanized fraction.

Catchment characteristics play an important regulating role in flood changes (Tanoue et al., 2016). Overall, stations with SID in multidimensional floods are more likely to occur in the catchments with low elevation, higher latitude, low slopes, and/or high urbanization. In contrast, stations with SDT in multidimensional floods are usually in the catchments with high aridity indexes, high elevation, and/or high irrigation fraction (Figures 11, S4 and S5).

5 Discussion and conclusions

Although the impacts of flood disasters have risen in recent decades (Tanoue et al., 2016), the question of whether floods in different dimensions (e.g., magnitude, frequency, and duration) are increasing remains largely unanswered at the global level. A greater frequency (but not a greater amount) of floods has been detected in the central United States (Mallakpourand Villarini, 2015). However, a little evidence for increasing trends in flood frequency has been found in other regions around the globe. Therefore, the results of this study provide a systematic update to flood changes across the globe. Comparing existing global assessments (Do et al., 2017; Gudmundsson

et al., 2019), the key progress resulting from this study is the consideration of multidimensional flood behaviors, as well as both the sign and magnitude of the trends; Moreover, the possible mechanisms of flood changes were investigated.

The global assessment highlights that spatial patterns in the signs of trends are generally consistent across multidimensional flood behaviors, with larger magnitude, more frequent and longer in duration in some regions but smaller, less frequent and shorter in other regions. This finding largely agrees with the previous study (Gudmundsson et al., 2019), which shows that the entire streamflow distribution is changing upward or downward for different regions worldwide. For flood magnitude, there are more stations showing SDT than SIT, which is consistent with the results of previous studies (Do et al., 2017; Kundzewicz et al., 2014). However, for flood frequency, significantly increasing trends were detected in more stations. From a global perspective, this result verified the argument from Hirsch and Archfield (2015) that floods tend to be more frequent rather than larger in central United States.

It is worth to mention that observed multidimensional flood trends may not continue in the future, since these changes may be also caused by the climate variability and human activities, rather than persistent climate change (Hodgkins et al., 2017). In addition, since the observed trends depend on the record period, the changing features of global floods may be different if the record period changed (Bloschl et al., 2019; Hall et al., 2014). However, our results are broadly consistent with previous studies in terms of regional flood changes and projected climate changes. For examples, previous studies have reported increasing floods in northern Europe (Bloeschl et al., 2017) and northern Australia (Liuand Zhang, 2017), while more decreasing floods were found in western North America (Whitfield, 2001) and southern Australia (Liuand Zhang, 2017). In addition, global climate models from CMIP5 ensemble suggest that the wetting

conditions with the global warming were projected in many regions, such as northern North America, southern Brazil, northern Europe (Greve et al., 2018); however, increasing drying conditions were detected in southern North America, eastern Brazil, northern Mediterranean, southern Arica, and southern Australia (Greve et al., 2018). These results from isolated regional floods studies and global climate projections are broadly consistent with our findings.

A clear spatiotemporal mismatch was detected globally between heavy precipitation and flood changes, that is, more increases in magnitude and frequency of heavy precipitation and the lack of corresponding increases in floods, even with outnumbered stations showing decreasing floods in most cases. Consequently, heavy precipitation is a crucial cause of flood formation but not flood changes. This finding implies that other hydroclimatic factors play a more important role in flood changes. Our findings reveal that globally multidimensional flood behaviors can be largely attributed to shifts in atmospheric circulation, TWSC, and dams' regulation, as well as the impacts of reducing the antecedent moisture deduction through warming temperature, with land use changes regulating the flood response.

The main limitation of this study is that the uneven distributed stations over the world and different temporal coverage of streamflow records for different stations, which may affect the results in the regional and global assessment to a certain degree. In addition, we investigate the the possible sources of the spatiotemporal changes in floods by qualitatively, rather than a quantitative attribution. However, the results of this study present an unprecedented insight into global-scale changes in multidimensional flood behaviors as well as their potential mechanisms. The results of this study are helpful for increasing our understanding of flood changes and their causes for climate change impact assessments and flood disaster prevention.

Acknowledgements:

We would like to thank the following organizations for providing streamflow data: the United States Geological Survey (USGS), the GRDC, the Brazilian Agência Nacional de Águas, EURO-FRIEND-Water, the Water Survey of Canada (WSC), the Australian Bureau of Meteorology (BoM), and the Chilean Center for Climate and Resilience Research (CR2). This study was supported by the China Postdoctoral Science Foundation funded project (BX20190301), Nature Science Foundation of Hubei Province (2019CFB221), Fundamental Research Funds for the Central Universities, China University of Geosciences (Wuhan) (162301182729), CAS Pioneer Hundred Talents Program and IGSNRR Supporting Fund (YJRCPT2019-101), the National Natural Science Foundation of China (U1911205 and 41901041), and the fund for the State Key Laboratory of Simulation and Regulation of Water Cycle in River Basin (Grant IWHR-SKL-KF201919). The authors declare that they have no conflicts of interest. The data supporting the conclusions of this study can be obtained from the website listed in the Data section and Table 1.

References

Alvarez-Garreton, C., Mendoza, P. A., Boisier, J. P., Addor, N., Hydrology, A. A. J., & Discussions, E. S. S. (2018). The CAMELS-CL dataset: catchment attributes and meteorology for large sample studies – Chile dataset, 1-40.

Archfield, S. A., Hirsch, R. M., Viglione, A., & Bloeschl, G. (2016). Fragmented patterns of flood change across the United States. *Geophysical Research Letters*, *43*(19), 10232-10239. doi:10.1002/2016gl070590

Asadieh, B., & Krakauer, N. Y. (2015). Global trends in extreme precipitation: climate models versus observations. *Hydrology and Earth System Sciences*, *19*(2), 877-891. doi:10.5194/hess-19-877-2015

Beck, H. E., Wood, E. F., Pan, M., Fisher, C. K., Miralles, D. G., van Dijk, A., McVicar, T. R., & Adler, R. F. (2019). MSWEP V2 Global 3-Hourly 0.1 degrees Precipitation: Methodology and Quantitative Assessment. *Bulletin of the American Meteorological Society*, *100*(3), 473-502. doi:10.1175/bams-d-17-0138.1

458 Berghuijs, W. R., Woods, R. A., Hutton, C. J., & Sivapalan, M. (2016). Dominant flood generating mechanisms
459 across the United States. *Geophysical Research Letters*, *43*(9), 4382-4390. doi:10.1002/2016gl068070
460 Bloeschl, G., et al. (2017). Changing climate shifts timing of European floods. *Science*, *357*(6351), 588-590.
461 doi:10.1126/science.aan2506
462 Bloschl, G., et al. (2019). Changing climate both increases and decreases European river floods. *Nature*, *573*(7772),
463 108-111. doi:10.1038/s41586-019-1495-6
464 Buermann, W., Dong, J., Zhou, L., & Myneni, R. B. J. J. o. G. R. (2002). Analysis of a Multi-year Global Vegetation
465 Leaf Area Index Data Set, *107*(D22), ACL-1-ACL 14-16.
466 Chang, W., Stein, M. L., Wang, J., Kotamarthi, V. R., & Moyer, E. J. (2016). Changes in Spatiotemporal
467 Precipitation Patterns in Changing Climate Conditions. *Journal of Climate*, *29*(23), 8355-8376.
468 doi:10.1175/jcli-d-15-0844.1
469 CRED (2015). The Human Cost of Natural Disasters: A Global Perspective. *Centre for Research on the*
470 *Epidemiology of Disasters, Brussels.*
471 Delgado, J. M., Apel, H., & Merz, B. (2010). Flood trends and variability in the Mekong river. *Hydrology and Earth*
472 *System Sciences*, *14*(3), 407-418. doi:10.5194/hess-14-407-2010
473 Do, H. X., Westra, S., & Leonard, M. (2017). A global-scale investigation of trends in annual maximum streamflow.
474 *Journal of Hydrology*, *552*, 28-43. doi:10.1016/j.jhydrol.2017.06.015
475 Donat, M. G., Lowry, A. L., Alexander, L. V., O'Gorman, P. A., & Maher, N. (2016). More extreme precipitation in
476 the world's dry and wet regions. *Nature Climate Change*, *6*(5), 508-513. doi:10.1038/nclimate2941
477 Doocy, S., Daniels, A., Murray, S., & Kirsch, T. D. J. P. C. (2013). The human impact of floods: a historical review
478 of events 1980-2009 and systematic literature review, *5*(5), 1808-1815.
479 Falcone, J. A., Carlisle, D. M., Wolock, D. M., & Meador, M. R. J. E. (2010). GAGES: A stream gage database for
480 evaluating natural and altered flow conditions in the conterminous United States, *91*(2), 621-621.
481 Fanta, B., Zaake, B. T., & Kachroo, R. K. (2001). A study of variability of annual river flow of the southern African
482 region. *Hydrological Sciences Journal-Journal Des Sciences Hydrologiques*, *46*(4), 513-524.
483 doi:10.1080/02626660109492847
484 Greve, P., Gudmundsson, L., & Seneviratne, S. I. (2018). Regional scaling of annual mean precipitation and water
485 availability with global temperature change. *Earth System Dynamics*, *9*(1), 227-240. doi:10.5194/esd-9-227-

2018

Gu, X., Zhang, Q., Li, J., Singh, V. P., Liu, J., Sun, P., He, C., & Wu, J. (2019a). Intensification and Expansion of Soil Moisture Drying in Warm Season Over Eurasia Under Global Warming. *Journal of Geophysical Research: Atmospheres*, *124*(7), 3765-3782. doi:10.1029/2018jd029776

Gu, X. H., Zhang, Q., Li, J. F., Singh, V. P., Liu, J. Y., Sun, P., & Cheng, C. X. (2019b). Attribution of Global Soil Moisture Drying to Human Activities: A Quantitative Viewpoint. *Geophysical Research Letters*, *46*(5), 2573-2582. doi:10.1029/2018gl080768

Gu, X. H., Zhang, Q., Li, J. F., Singh, V. P., & Sun, P. (2019c). Impact of urbanization on nonstationarity of annual and seasonal precipitation extremes in China. *Journal of Hydrology*, *575*, 638-655. doi:10.1016/j.jhydrol.2019.05.070

Gudmundsson, L., Greve, P., & Seneviratne, S. I. (2017). Correspondence: Flawed assumptions compromise water yield assessment. *Nat Commun*, *8*, 14795. doi:10.1038/ncomms14795

Gudmundsson, L., Leonard, M., Do, H. X., Westra, S., & Seneviratne, S. I. (2019). Observed Trends in Global Indicators of Mean and Extreme Streamflow. *Geophysical Research Letters*, *46*(2), 756-766. doi:10.1029/2018gl079725

Hall, J., et al. (2014). Understanding flood regime changes in Europe: a state-of-the-art assessment. *Hydrology and Earth System Sciences*, *18*(7), 2735-2772. doi:10.5194/hess-18-2735-2014

Hannaford, J., Buys, G., Stahl, K., & Tallaksen, L. M. (2013). The influence of decadal-scale variability on trends in long European streamflow records. *Hydrology and Earth System Sciences*, *17*(7), 2717-2733. doi:10.5194/hess-17-2717-2013

Hensel, D. R., & Frans, L. M. (2006). Regional Kendall test for trend. *Environmental Science & Technology*, *40*(13), 4066-4073. doi:10.1021/es051650b

Hettiarachchi, S., Wasko, C., & Sharma, A. (2018). Increase in flood risk resulting from climate change in a developed urban watershed - the role of storm temporal patterns. *Hydrology and Earth System Sciences*, *22*(3), 2041-2056. doi:10.5194/hess-22-2041-2018

Hirsch, R. M., & Archfield, S. A. (2015). Not higher but more often. *Nature Climate Change*, *5*(3), 198-199. doi:10.1038/nclimate2551

Hirsch, R. M., & Slack, J. R. (1984). A NONPARAMETRIC TREND TEST FOR SEASONAL DATA WITH

514 SERIAL DEPENDENCE. *Water Resources Research*, *20*(6), 727-732. doi:10.1029/WR020i006p00727
515 Hodgkins, G. A., Dudley, R. W., Archfield, S. A., & Renard, B. (2019). Effects of climate, regulation, and
516 urbanization on historical flood trends in the United States. *Journal of Hydrology*, *573*, 697-709.
517 doi:10.1016/j.jhydrol.2019.03.102
518 Hodgkins, G. A., et al. (2017). Climate-driven variability in the occurrence of major floods across North America
519 and Europe. *Journal of Hydrology*, *552*, 704-717. doi:10.1016/j.jhydrol.2017.07.027
520 Ishak, E. H., Rahman, A., Westra, S., Sharma, A., & Kuczera, G. (2013). Evaluating the non-stationarity of
521 Australian annual maximum flood. *Journal of Hydrology*, *494*, 134-145. doi:10.1016/j.jhydrol.2013.04.021
522 Ivancic, T. J., & Shaw, S. B. (2015). Examining why trends in very heavy precipitation should not be mistaken for
523 trends in very high river discharge. *Climatic Change*, *133*(4), 681-693. doi:10.1007/s10584-015-1476-1
524 Johnson, F., White, C. J., van Dijk, A., Ekstrom, M., Evans, J. P., Jakob, D., Kiem, A. S., Leonard, M., Rouillard, A.,
525 & Westra, S. (2016). Natural hazards in Australia: floods. *Climatic Change*, *139*(1), 21-35.
526 doi:10.1007/s10584-016-1689-y
527 Kalnay, E., Kanamitsu, M., Kistler, R., Collins, W., Deaven, D., Gandin, L., Iredell, M., Saha, S., White, G., &
528 Woollen, J. (1996). The NCEP/NCAR 40-year reanalysis project. *Bulletin of the American meteorological*
529 *Society*, *77*(3), 437-471.
530 Kiktev, D., Sexton, D. M. H., Alexander, L., & Folland, C. K. (2003). Comparison of modeled and observed trends
531 in indices of daily climate extremes. *Journal of Climate*, *16*(22), 3560-3571. doi:10.1175/1520-
532 0442(2003)016<3560:Comaot>2.0.Co;2
533 Kundzewicz, Z. W., et al. (2014). Flood risk and climate change: global and regional perspectives. *Hydrological*
534 *Sciences Journal-Journal Des Sciences Hydrologiques*, *59*(1), 1-28. doi:10.1080/02626667.2013.857411
535 Lee, D., Ward, P., & Block, P. (2018). Attribution of Large-Scale Climate Patterns to Seasonal Peak-Flow and
536 Prospects for Prediction Globally. *Water Resources Research*, *54*(2), 916-938. doi:10.1002/2017wr021205
537 Lehmann, J., Mempel, F., & Coumou, D. (2018). Increased Occurrence of Record-Wet and Record-Dry Months
538 Reflect Changes in Mean Rainfall. *Geophysical Research Letters*, *45*(24), 13,468-413,476.
539 doi:10.1029/2018gl079439
540 Liu, J., Zhang, Q., Singh, V. P., Gu, X., & Shi, P. (2017). Nonstationarity and clustering of flood characteristics and
541 relations with the climate indices in the Poyang Lake basin, China. *Hydrological Sciences Journal-Journal Des*

Sciences Hydrologiques, *62*(11), 1809-1824. doi:10.1080/02626667.2017.1349909

Liu, J., & Zhang, Y. (2017). Multi-temporal clustering of continental floods and associated atmospheric circulations. *Journal of Hydrology*, *555*, 744-759. doi:10.1016/j.jhydrol.2017.10.072

Liu, J., Zhang, Y., Yang, Y., Gu, X., & Xiao, M. (2018). Investigating Relationships Between Australian Flooding and Large-Scale Climate Indices and Possible Mechanism. *Journal of Geophysical Research: Atmospheres*, *123*(16), 8708-8723. doi:10.1029/2017jd028197

Long, D., Shen, Y. J., Sun, A., Hong, Y., Longuevergne, L., Yang, Y. T., Li, B., & Chen, L. (2014). Drought and flood monitoring for a large karst plateau in Southwest China using extended GRACE data. *Remote Sensing of Environment*, *155*, 145-160. doi:10.1016/j.rse.2014.08.006

Lu, M., Lall, U., Schwartz, A., & Kwon, H. (2013). Precipitation predictability associated with tropical moisture exports and circulation patterns for a major flood in France in 1995. *Water Resources Research*, *49*(10), 6381-6392. doi:10.1002/wrcr.20512

Mallakpour, I., & Villarini, G. (2015). The changing nature of flooding across the central United States. *Nature Climate Change*, *5*(3), 250-254. doi:10.1038/nclimate2516

Mallakpour, I., & Villarini, G. (2016). Investigating the relationship between the frequency of flooding over the central United States and large-scale climate. *Advances in Water Resources*, *92*, 159-171. doi:10.1016/j.advwatres.2016.04.008

Marchetto, A., Rogora, M., & Arisci, S. (2013). Trend analysis of atmospheric deposition data: A comparison of statistical approaches. *Atmos. Environ.*, *64*, 95-102. doi:10.1016/j.atmosenv.2012.08.020

Marengo, J. A., Tomasella, J., & Uvo, C. R. (1998). Trends in streamflow and rainfall in tropical South America: Amazonia, eastern Brazil, and northwestern Peru. *Journal of Geophysical Research-Atmospheres*, *103*(D2), 1775-1783. doi:10.1029/97jd02551

Milly, P. C. D., Wetherald, R. T., Dunne, K. A., & Delworth, T. L. (2002). Increasing risk of great floods in a changing climate. *Nature*, *415*(6871), 514-517. doi:10.1038/415514a

Musselman, K. N., Lehner, F., Ikeda, K., Clark, M. P., Prein, A. F., Liu, C., Barlage, M., & Rasmussen, R. (2018). Projected increases and shifts in rain-on-snow flood risk over western North America. *Nature Climate Change*, *8*(9), 808-817. doi:10.1038/s41558-018-0236-4

Najibi, N., Devineni, N., Lu, M., & Perdigão, R. A. P. (2019). Coupled flow accumulation and atmospheric blocking

govern flood duration. *npj Climate and Atmospheric Science*, *2*(1). doi:10.1038/s41612-019-0076-6

Niu, J., Shen, C. P., Li, S. G., & Phanikumar, M. S. (2014). Quantifying storage changes in regional Great Lakes watersheds using a coupled subsurface-land surface process model and GRACE, MODIS products. *Water Resources Research*, *50*(9), 7359-7377. doi:10.1002/2014wr015589

Payero, J. O., Tarkalson, D. D., Irmak, S., Davison, D., & Petersen, J. L. (2008). Effect of irrigation amounts applied with subsurface drip irrigation on corn evapotranspiration, yield, water use efficiency, and dry matter production in a semiarid climate. *Agricultural Water Management*, *95*(8), 895-908. doi:10.1016/j.agwat.2008.02.015

Reager, J. T., Thomas, B. F., & Famiglietti, J. S. (2014). River basin flood potential inferred using GRACE gravity observations at several months lead time. *Nature Geoscience*, *7*(8), 589-593. doi:10.1038/ngeo2203

Sharma, A., Wasko, C., & Lettenmaier, D. P. (2018). If Precipitation Extremes Are Increasing, Why Aren't Floods? *Water Resources Research*, *54*(11), 8545-8551. doi:10.1029/2018wr023749

Sheffield, J., & Wood, E. F. (2008). Global trends and variability in soil moisture and drought characteristics, 1950-2000, from observation-driven Simulations of the terrestrial hydrologic cycle. *Journal of Climate*, *21*(3), 432-458. doi:10.1175/2007jcli1822.1

Sheng, Y., & Wang, L. (2012). Detection of Changes, Changes in Flood Risk in Europe. *CRC Press*, 387-408. doi:http://dx.doi.org/10.1201/b12348-26

Sillmann, J., Kharin, V. V., Zwiers, F. W., Zhang, X., & Bronaugh, D. (2013). Climate extremes indices in the CMIP5 multimodel ensemble: Part 2. Future climate projections. *Journal of Geophysical Research-Atmospheres*, *118*(6), 2473-2493. doi:10.1002/jgrd.50188

Slater, L. J., & Villarini, G. (2016). Recent trends in US flood risk. *Geophysical Research Letters*, *43*(24), 12428-12436. doi:10.1002/2016gl071199

Stahl, K., Hisdal, H., Hannaford, J., Tallaksen, L. M., van Lanen, H. A. J., Sauquet, E., Demuth, S., Fendekova, M., & Jodar, J. (2010). Streamflow trends in Europe: evidence from a dataset of near-natural catchments. *Hydrology and Earth System Sciences*, *14*(12), 2367-2382. doi:10.5194/hess-14-2367-2010

Stahl, K., Tallaksen, L. M., Hannaford, J., & van Lanen, H. A. J. (2012). Filling the white space on maps of European runoff trends: estimates from a multi-model ensemble. *Hydrology and Earth System Sciences*, *16*(7), 2035-2047. doi:10.5194/hess-16-2035-2012

598 Tananaev, N. I., Makarieva, O. M., & Lebedeva, L. S. (2016). Trends in annual and extreme flows in the Lena River
599 basin, Northern Eurasia. *Geophysical Research Letters*, *43*(20), 10764-10772. doi:10.1002/2016gl070796
600 Tanoue, M., Hirabayashi, Y., & Ikeuchi, H. (2016). Global-scale river flood vulnerability in the last 50 years. *Sci*
601 *Rep*, *6*, 36021. doi:10.1038/srep36021
602 Wasko, C., Pui, A., Sharma, A., Mehrotra, R., & Jeremiah, E. (2015). Representing low-frequency variability in
603 continuous rainfall simulations: A hierarchical random Bartlett Lewis continuous rainfall generation model.
604 *Water Resources Research*, *51*(12), 9995-10007. doi:10.1002/2015wr017469
605 Wasko, C., Sharma, A., & Westra, S. (2016). Reduced spatial extent of extreme storms at higher temperatures.
606 *Geophysical Research Letters*, *43*(8), 4026-4032. doi:10.1002/2016gl068509
607 Westra, S., Alexander, L. V., & Zwiers, F. W. (2013). Global Increasing Trends in Annual Maximum Daily
608 Precipitation. *Journal of Climate*, *26*(11), 3904-3918. doi:10.1175/jcli-d-12-00502.1
609 Whitfield, P. H. (2001). Linked hydrologic and climate variations in British Columbia and Yukon. *Environmental*
610 *Mo*nitoring and Assessment, 67(1-2), 217-238. doi:10.1023/a:1006438723879
611 Zhang, Y. Q., Viney, N., Frost, A., Oke, A., Brooks, M., Chen, Y., & Campbell, N. (2013). Collation of Australian
612 modeller's streamflow dataset for 780 unregulated Australian catchments. Water for a Healthy Country
613 National Research Flagship. doi:https://doi.org/10.4225/08/58b5baad4fcc2
614
615

Figure 1. Maps showing the information of (**a-e**) global 21,955 hydrological stations and (**f**) the selected 6,852 stations.

Figure 2. Maps of trends in the flood magnitude, frequency and duration. The red (blue) triangles represent the stations showing significantly increasing (decreasing) trends at the 95% confidence level.

Figure 3. The percentages of stations showing significantly increasing and decreasing trend in flood (**a-b**) magnitude, (**c-d**) frequency, and (**e-f**) duration. The histogram shows the percentages distribution of stations with significant trend obtained by 2000 bootstrap sampling. The dark gray dashed lines indicated the 95th percentile of percentages distribution. The red dots represent the percentages based on the observed dataset.

Figure 4. Maps for regional-mean changes (%/decade) in flood magnitude, frequency and duration. The 'S' symbols represent regions with a significant trend at the 95% confidence level.

Figure 5. Maps for the trends in heavy precipitation magnitude and frequency, mean precipitation and temperature. The red (blue) triangles indicate catchments with significant decreasing (increasing) trends at the 95% confidence level.

Figure 6. Maps for the correlations among floods, heavy precipitation and temperature. Only the stations with significant correlation were presented. The colors for points represent correlation coefficients. The histogram shows the percentages of stations with significantly positive and negative correlation by using red and blue colors, respectively.

Figure 7. Linear trends in the 850 hPa geopotential height (left panels) and horizontal wind (right panels) at the seasonal scale from 1960-2017 by using the NCEP/NCAR reanalysis data.

Figure 8. Maps showing the trends in flood magnitude, frequency and duration, alongside trends in terrestrial storage change (TWS) in cm/yr during 2003-2016. The area in red (blue) presents a decreasing (increasing) trend in TWSC. The red (blue) points represent the stations showing significantly increasing (decreasing) trends in floods at the 95% confidence level.

Figure 9. the same to figure 8, but for seasonal scale.

Figure 10. The percentages of dams-impact stations that showing significantly increasing and decreasing trend in flood (**a-b**) magnitude, (**c-d**) frequency, and (**e-f**) duration. The histogram shows the percentages distribution of stations with significant trend obtained by 2000 bootstrap sampling. The dark gray dashed lines indicated the 95th percentile of percentages distribution. The red dots represent the percentages based on the observed dataset.

Figure 11. The differences in the percentages of stations (excluding the stations affected by dams) with significantly increasing and decreasing trends in flood magnitudes under different catchment characteristics. The L, M and H denotes the values smaller than first third, between the first and second third, and larger than the last third for each catchment characteristic. The intervals indicate the 5% and 95% uncertainties.

Table 1. Global datasets used in extracting the catchment characteristics

Variables	Data sources	Spatial resolution
Irrigation	Global Map of Irrigation Areas (GMIA) (http://www.fao.org/nr/water/aquastat/irrigationmap/index10.stm)	5 arcmin× 5 arcmin
Land cover	ESA GlobCover Version 2.3 (https://www.edenextdata.com/?q=content/esa-	9 arcsec × 9 arcsec

	globcover-version-23-2009-300m-resolution-land-cover-map-0)	
NDVI	MODIS Vegetation Index Products (https://ecocast.arc.nasa.gov/data/pub/gimms/) (Buermann et al., 2002)	7.5 arcsec × 7.5 arcsec
Population	Gridded Population of the World (GPW) (http://sedac.ciesin.columbia.edu/data/set/gpw-v4-population-count)	30 arcsec × 30 arcsec
Slope and Elevation	GTOPO30 global digital elevation model (http://www.temis.nl/data/gtopo30.html) and ViewFinder DEM (http://viewfinderpanoramas.org/)	30 arcsec × 30 arcsec
Soil profile	Soil grid (https://soilgrids.org)	7.5 arcsec × 7.5 arcsec

659

660 **Table 2.** The percentage of stations showing significant increasing (decreasing) trends in flood
661 magnitude, frequency and duration for different regions.

NO.	Regions	LAB	Stations	Magnitude	Frequency	Duration
1	Alaska/N.W. Canada	ALA	112	4.5 (10.7)	8 (11.6)	10.7 (8)
2	Amazon	AMZ	148	13.5 (2.7)	11.5 (0)	10.1 (0.7)
3	Central Europe	CEU	526	12.7 (5.5)	5.7 (4.6)	7.8 (6.5)
4	Canada/Greenland/Iceland	CGI	133	17.3 (14.3)	15 (6.8)	29.3 (10.5)
5	Central North America	CNA	1153	8.8 (8.5)	11.2 (7.8)	17.5 (7.7)
6	East North America	ENA	1309	5.7 (7)	10.9 (5.1)	6 (7.5)
7	North Australia	NAU	195	2.6 (1)	0 (4.1)	4.6 (2.6)
8	North-East Brazil	NEB	377	2.7 (15.4)	2.7 (9.3)	2.7 (18.8)
9	North Europe	NEU	382	15.2 (2.9)	16.2 (1.8)	17.5 (2.1)
10	South Australia/New Zealand	SAU	395	1.5 (21.8)	2 (19.5)	1.8 (23)
11	Southeastern South America	SSA	382	13.6 (4.2)	9.9 (3.1)	10.2 (4.5)

12	West North America	WNA	1298	4.3 (13.9)	6.2 (10.4)	5.4 (11.6)
13	West Coast South America	WSA	163	3.1 (11.7)	6.1 (3.1)	1.8 (6.7)

662

Figure 1.

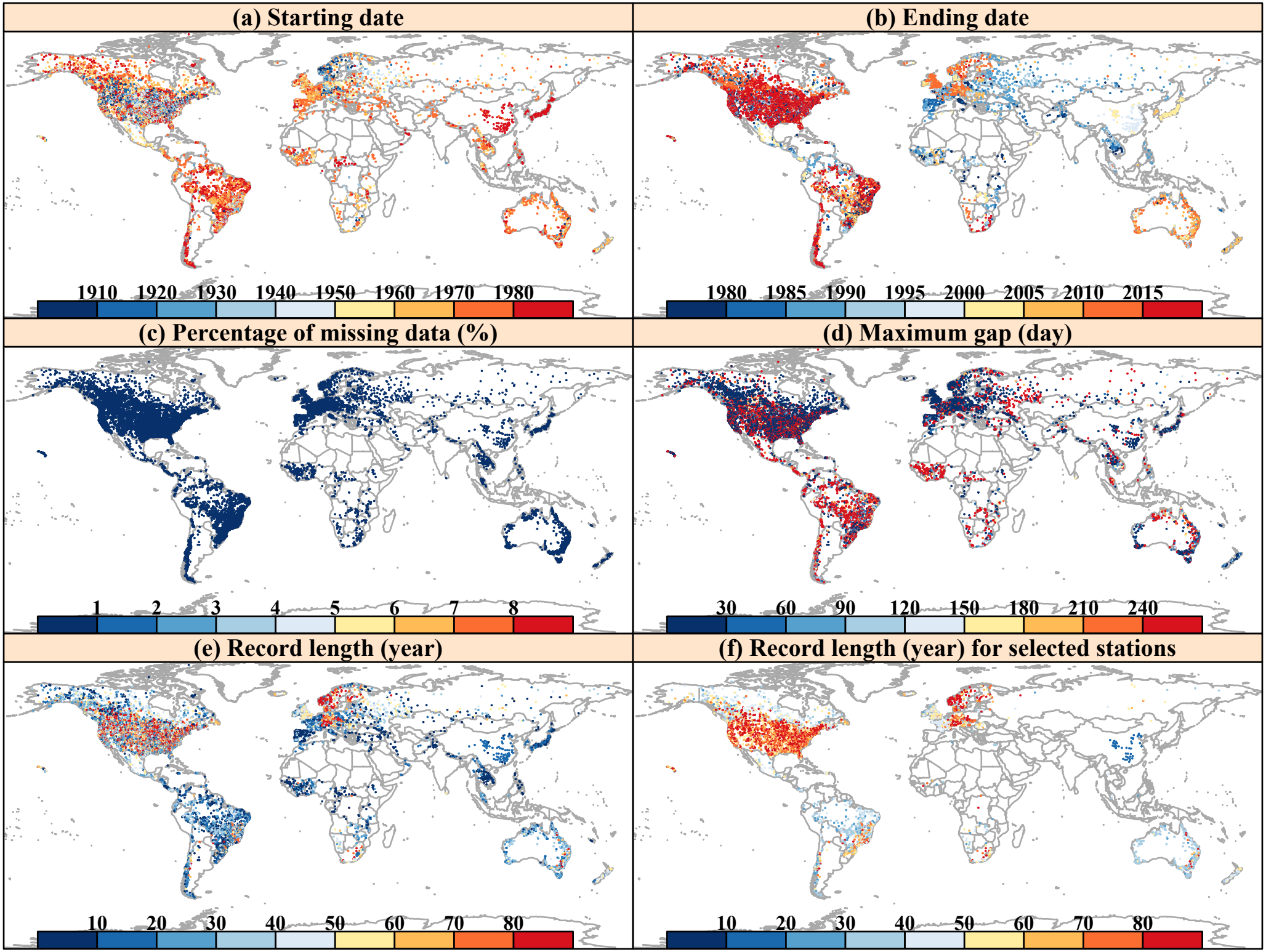
(a) Starting date
1910 1920 1930 1940 1950 1960 1970 1980
(b) Ending date
1980 1985 1990 1995 2000 2005 2010 2015
(c) Percentage of missing data (%)
1 2 3 4 5 6 7 8
(d) Maximum gap (day)
30 60 90 120 150 180 210 240
(e) Record length (year)
10 20 30 40 50 60 70 80
(f) Record length (year) for selected stations
10 20 30 40 50 60 70 80

Figure 2.

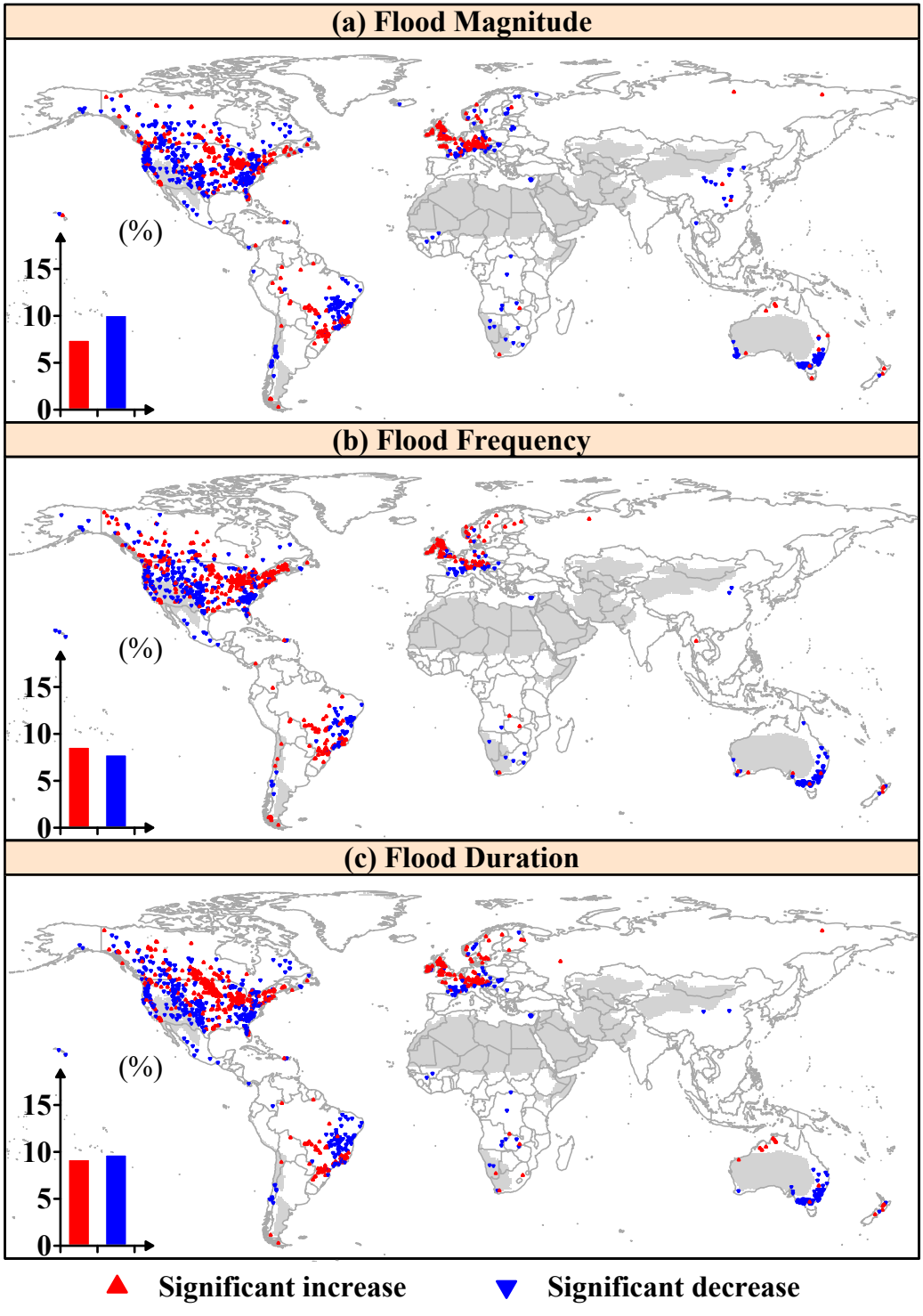
(a) Flood Magnitude
(%)
15
10
5
0
(b) Flood Frequency
(%)
15
10
5
0
(c) Flood Duration
(%)
15
10
5
0
Significant increase
Significant decrease

Figure 3.

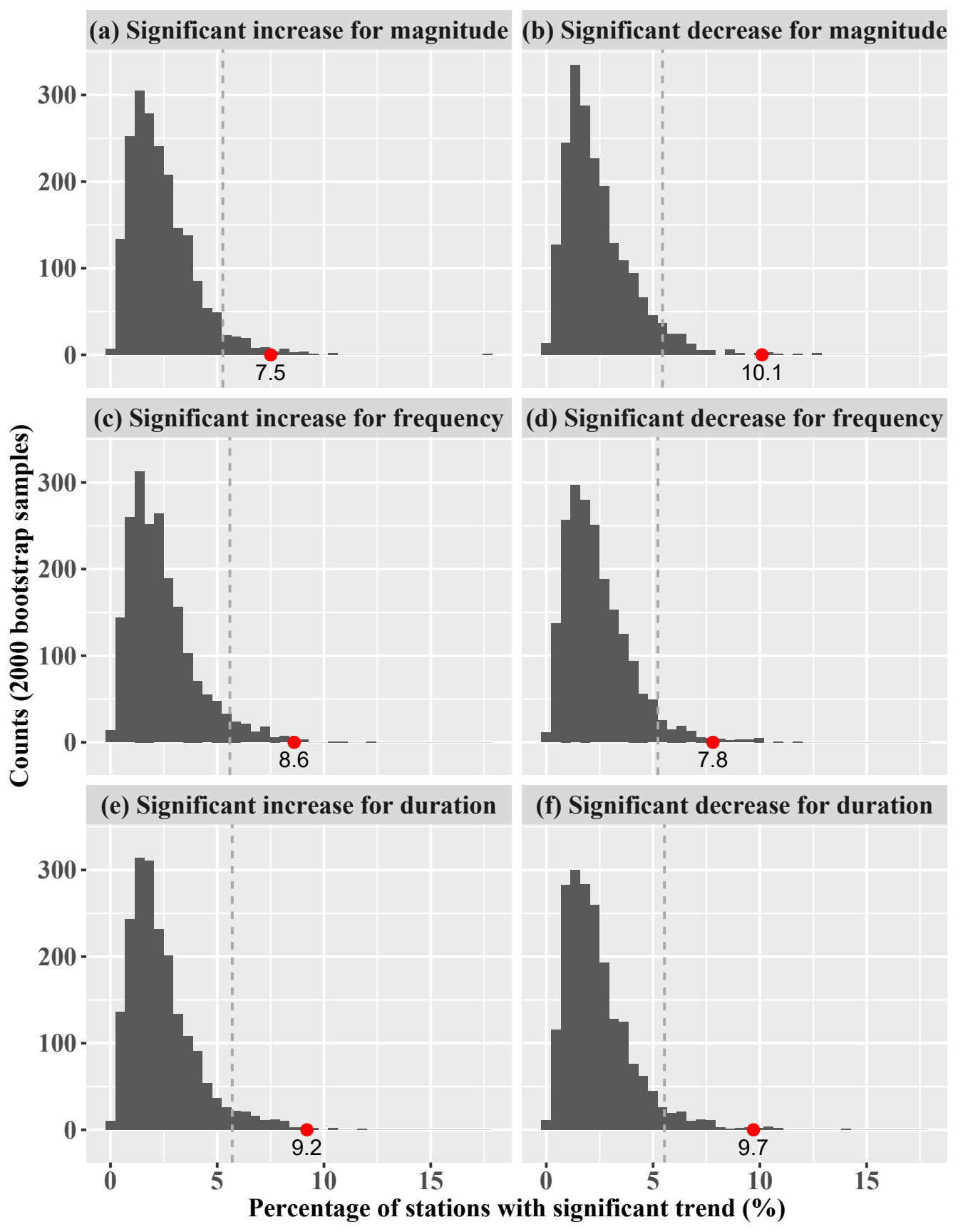
(a) Significant increase for magnitude
(b) Significant decrease for magnitude
(c) Significant increase for frequency
(d) Significant decrease for frequency
(e) Significant increase for duration
(f) Significant decrease for duration
7.5
10.1
8.6
7.8
9.2
9.7
300
200
100
0
0
5
10
15
Counts (2000 bootstrap samples)
Percentage of stations with significant trend (%)

Figure 4.

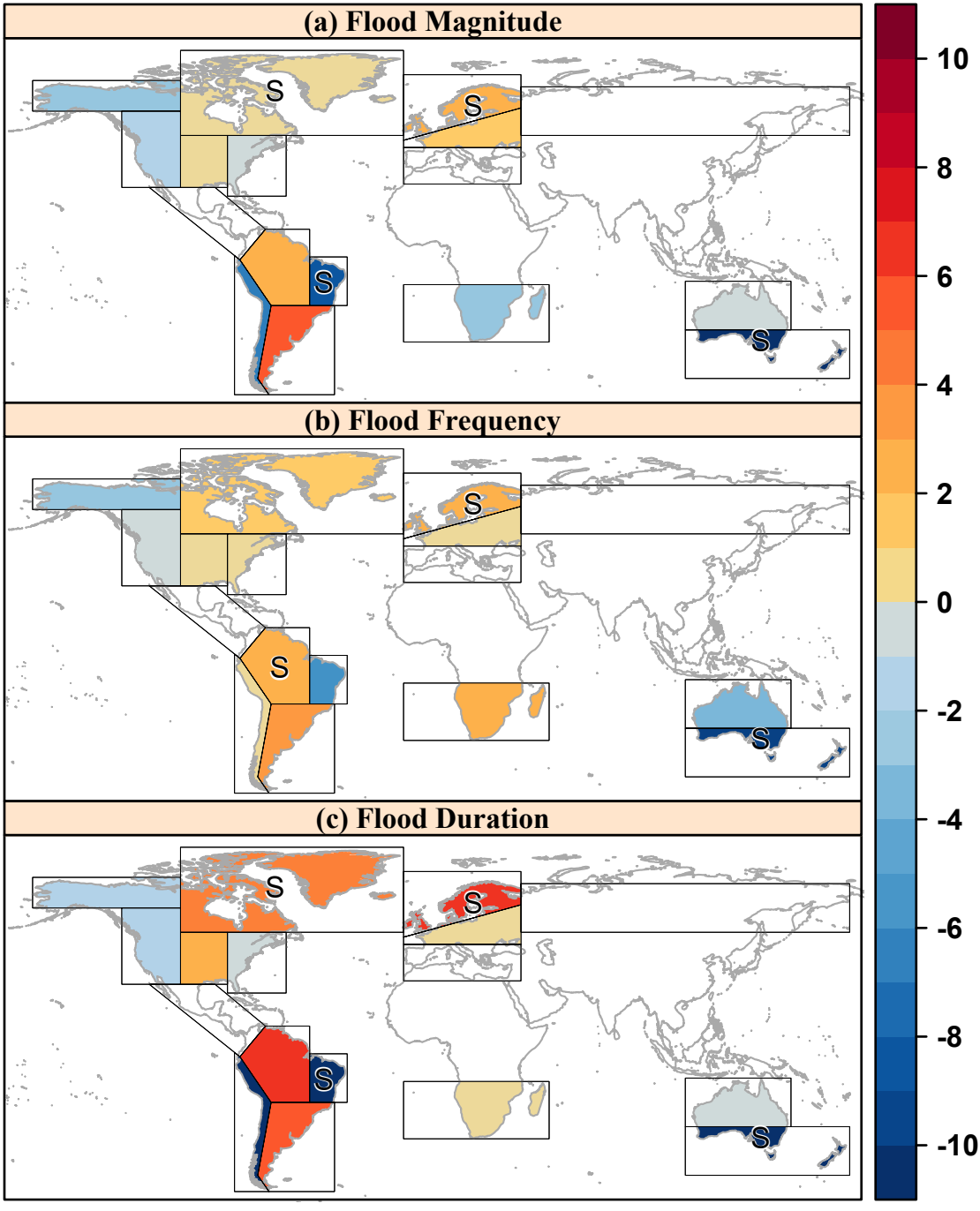
(a) Flood Magnitude
(b) Flood Frequency
(c) Flood Duration
S
10
8
6
4
2
0
-2
-4
-6
-8
-10

Figure 5.

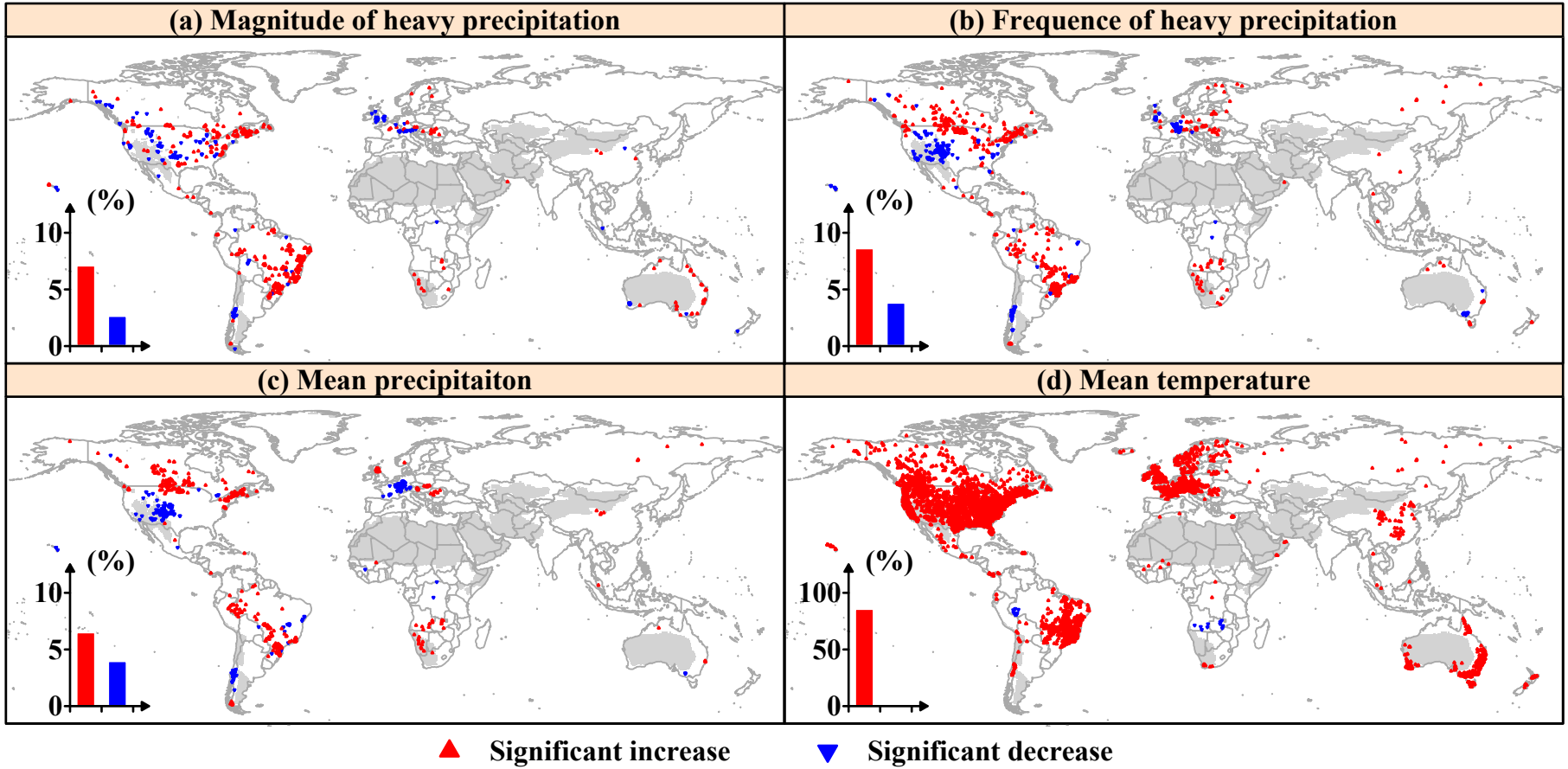
(a) Magnitude of heavy precipitation
(b) Frequence of heavy precipitation
(c) Mean precipitaiton
(d) Mean temperature
(%)
10
5
0
100
50
Significant increase
Significant decrease

Figure 6.

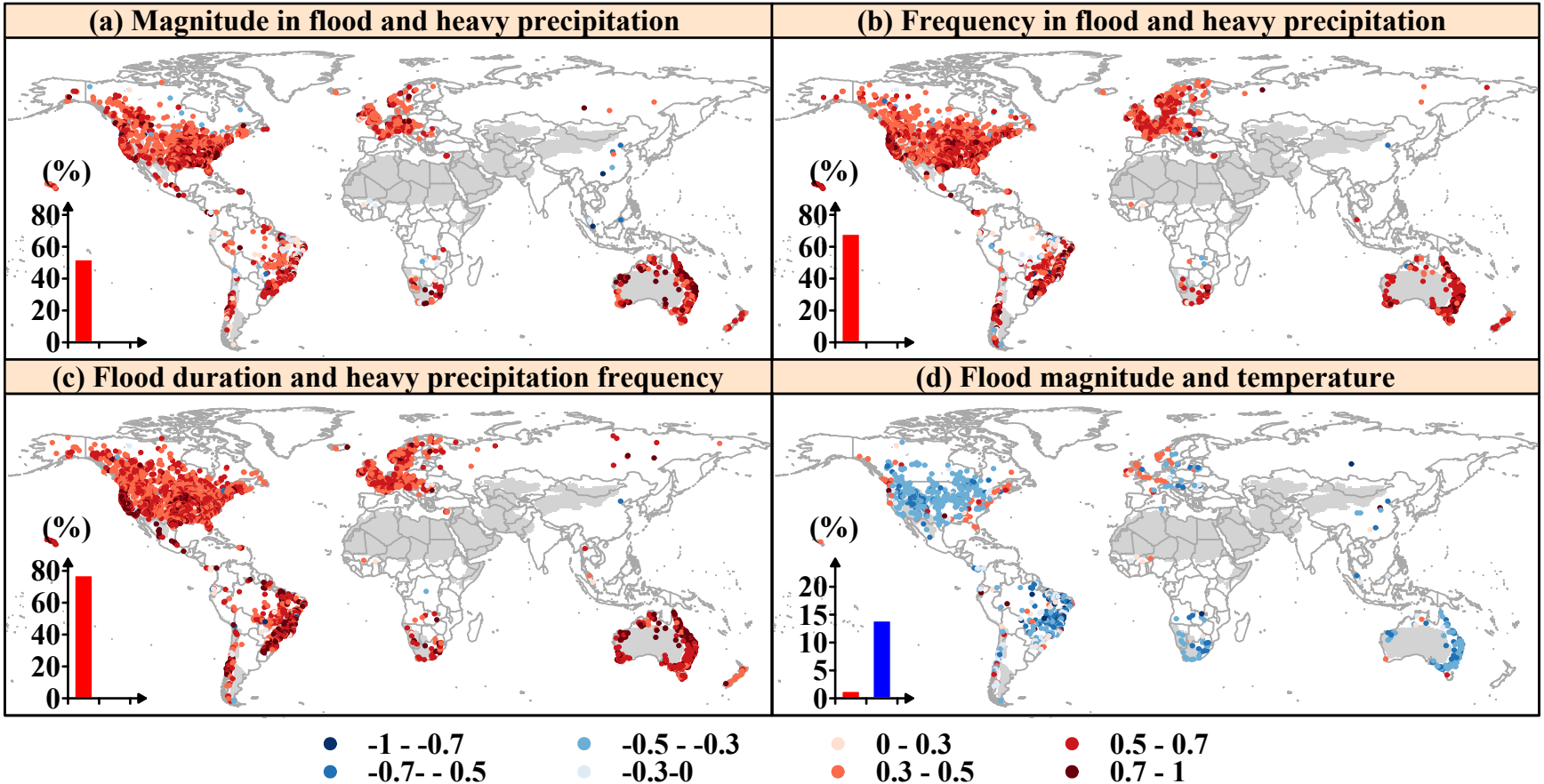
(a) Magnitude in flood and heavy precipitation
(b) Frequency in flood and heavy precipitation
(c) Flood duration and heavy precipitation frequency
(d) Flood magnitude and temperature
(%)
80
60
40
20
0
(%)
80
60
40
20
0
(%)
80
60
40
20
0
(%)
20
15
10
5
0
-1 - -0.7
-0.7- - 0.5
-0.5 - -0.3
-0.3-0
0 - 0.3
0.3 - 0.5
0.5 - 0.7
0.7 - 1

Figure 7.

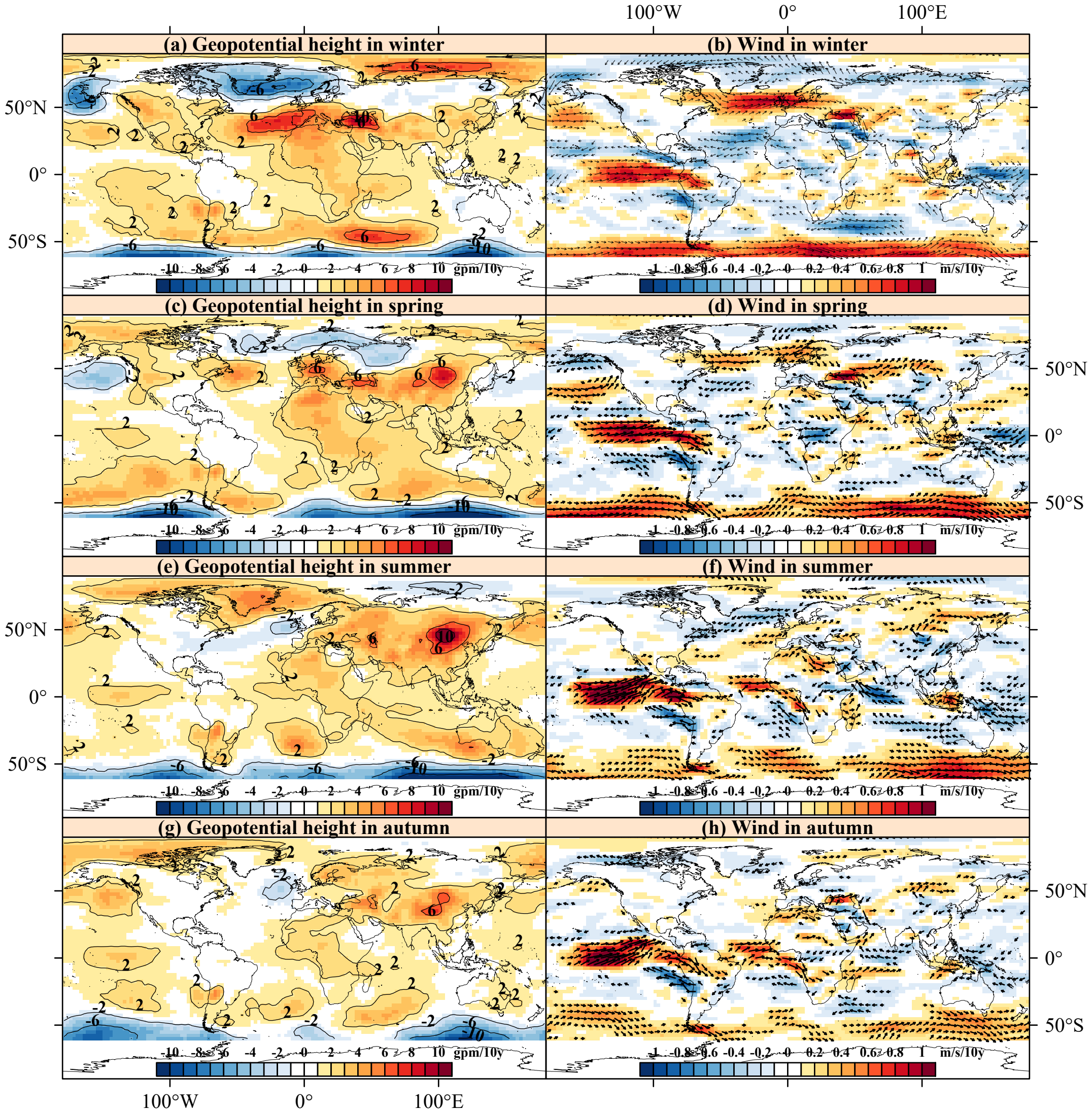
100°W
0°
100°E
50°N
0°
50°S
(a) Geopotential height in winter
(b) Wind in winter
(c) Geopotential height in spring
(d) Wind in spring
(e) Geopotential height in summer
(f) Wind in summer
(g) Geopotential height in autumn
(h) Wind in autumn
-10 -8 -6 -4 -2 0 2 4 6 8 10 gpm/10y
-1 -0.8 -0.6 -0.4 -0.2 0 0.2 0.4 0.6 0.8 1 m/s/10y

Figure 8.

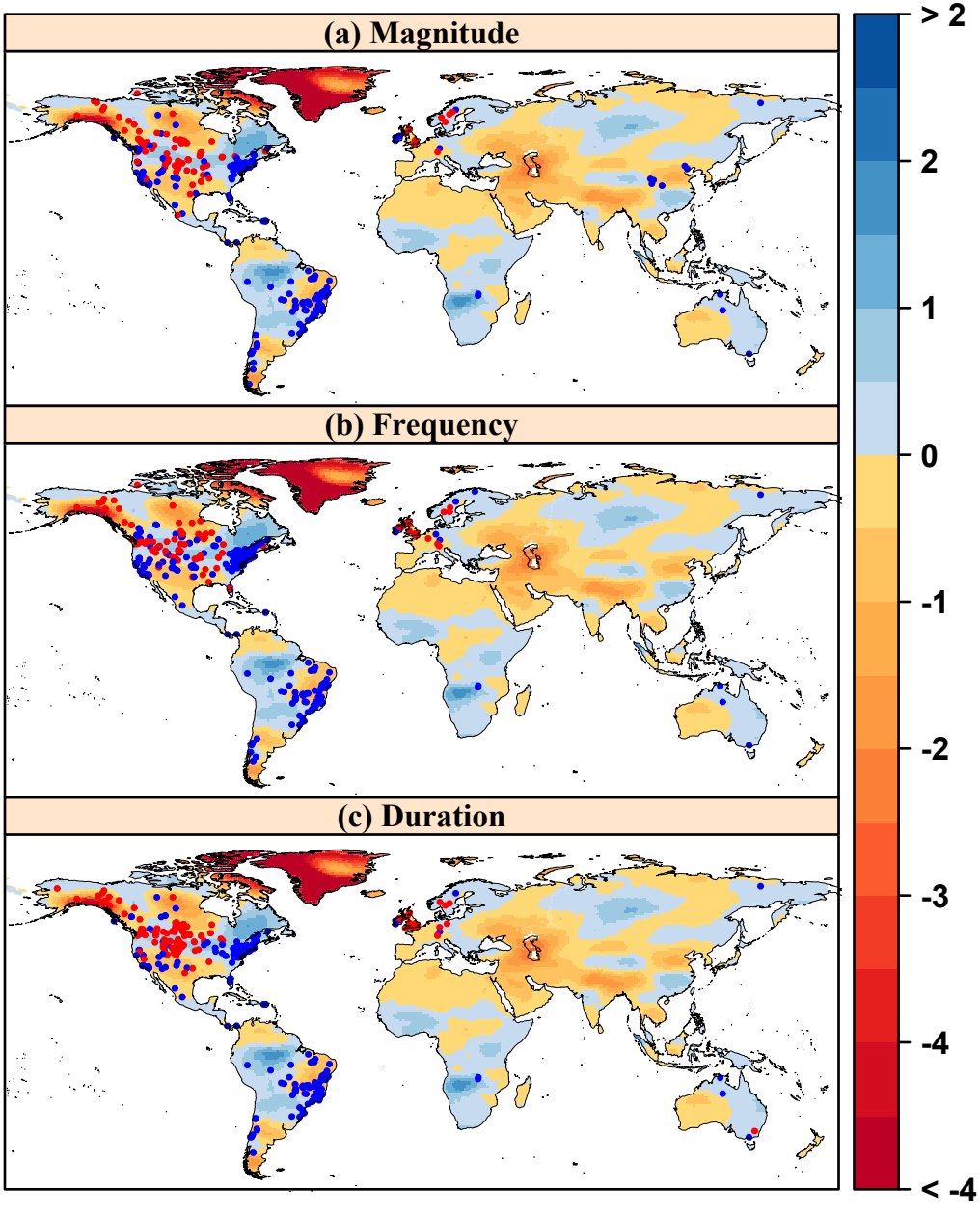
(a) Magnitude
(b) Frequency
(c) Duration
> 2
2
1
0
-1
-2
-3
-4
< -4

Figure 9.

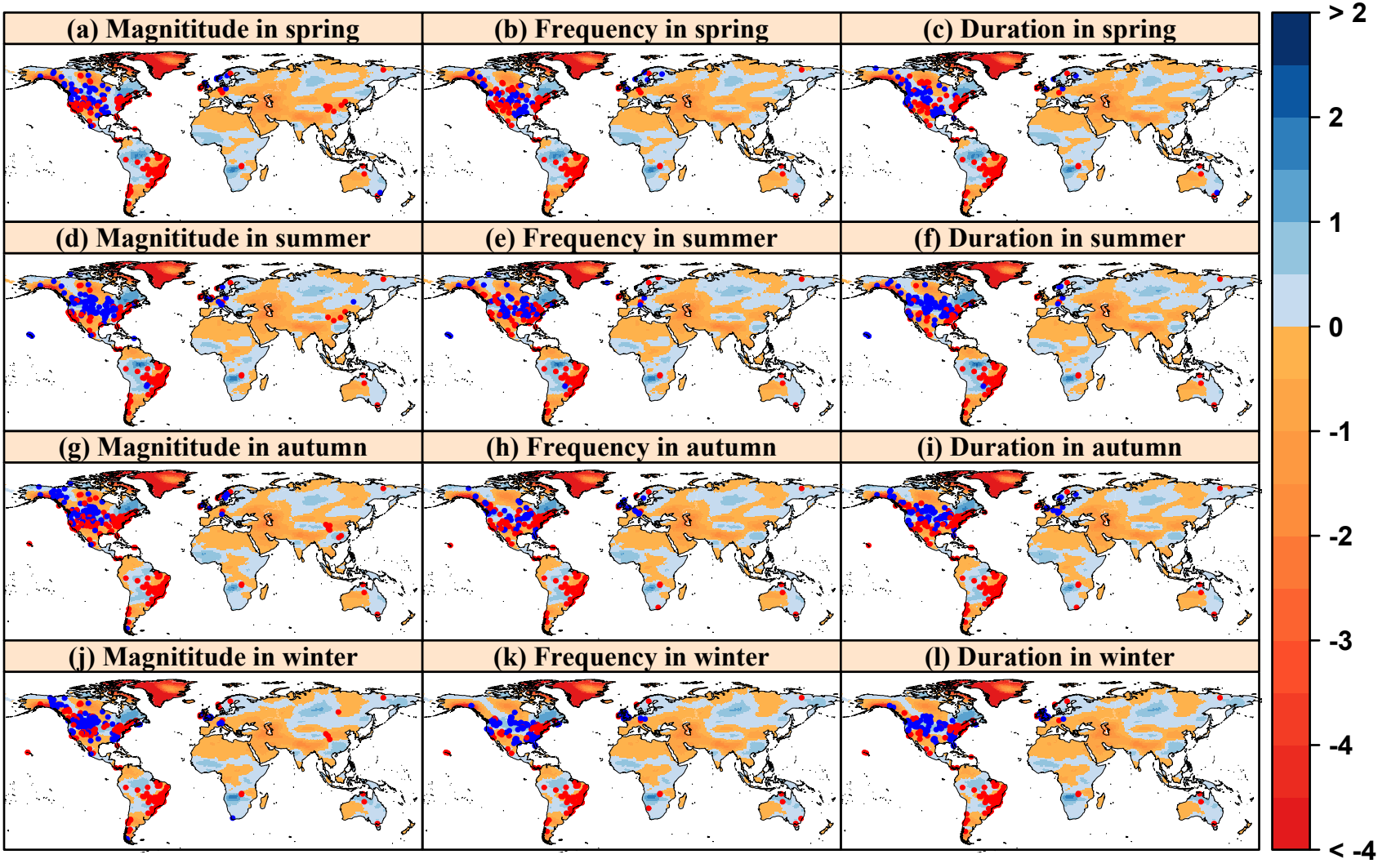
(a) Magnititude in spring
(b) Frequency in spring
(c) Duration in spring
(d) Magnititude in summer
(e) Frequency in summer
(f) Duration in summer
(g) Magnititude in autumn
(h) Frequency in autumn
(i) Duration in autumn
(j) Magnititude in winter
(k) Frequency in winter
(l) Duration in winter
> 2
2
1
0
-1
-2
-3
-4
< -4

Figure 10.

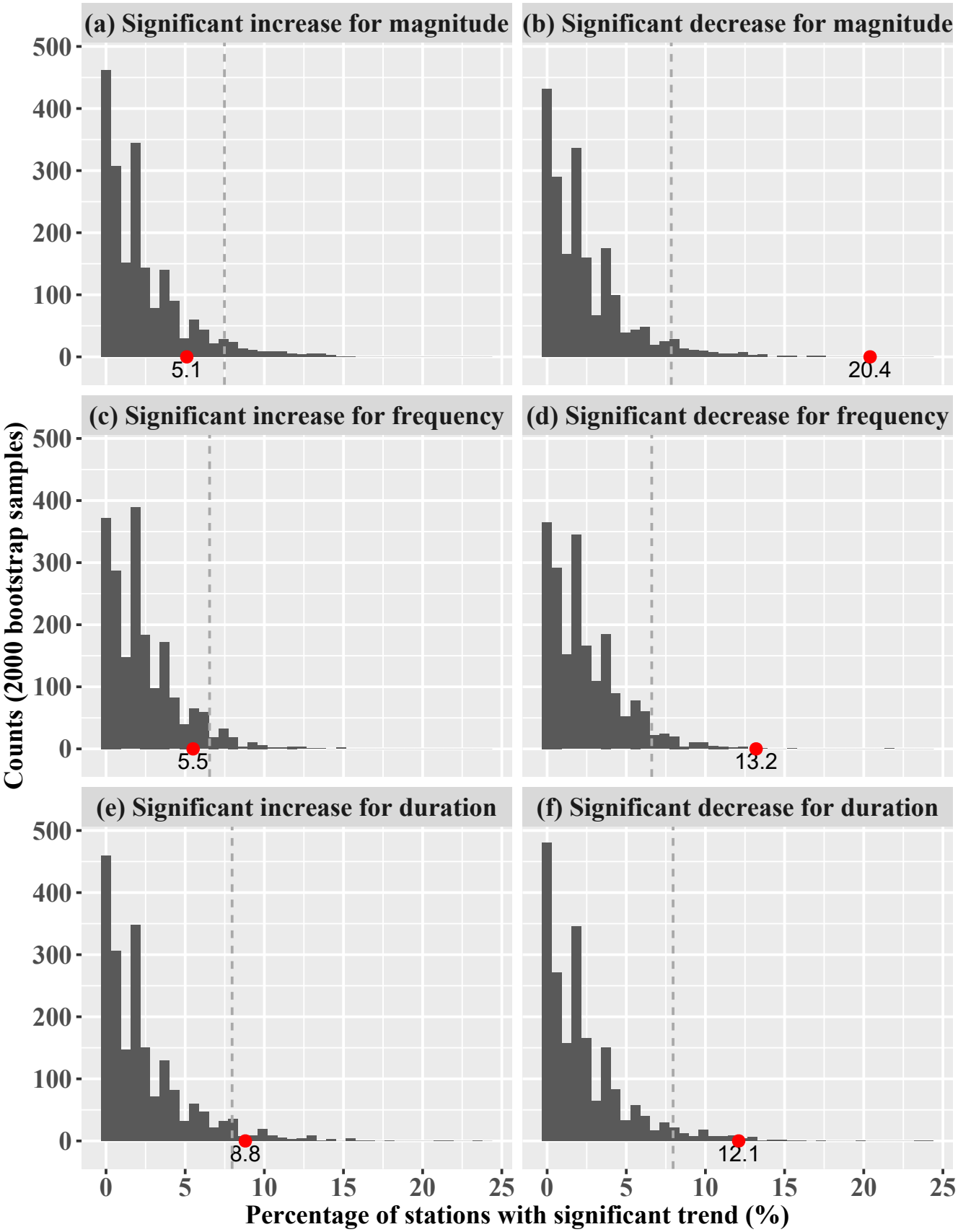
(a) Significant increase for magnitude
(b) Significant decrease for magnitude
(c) Significant increase for frequency
(d) Significant decrease for frequency
(e) Significant increase for duration
(f) Significant decrease for duration
5.1
20.4
5.5
13.2
8.8
12.1
Counts (2000 bootstrap samples)
Percentage of stations with significant trend (%)
0
100
200
300
400
500
0
5
10
15
20
25

Figure 11.

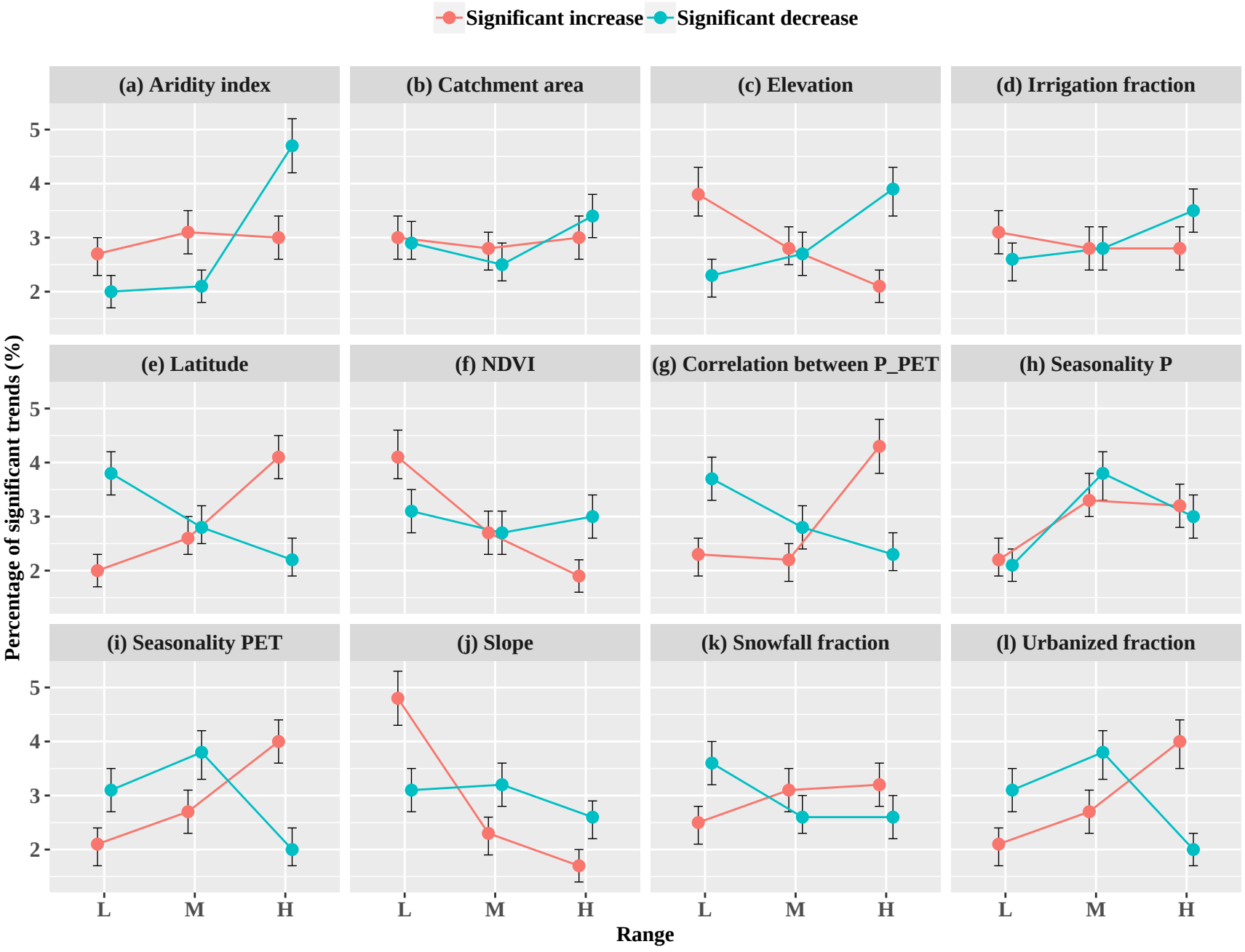
Significant increase
Significant decrease
(a) Aridity index
(b) Catchment area
(c) Elevation
(d) Irrigation fraction
(e) Latitude
(f) NDVI
(g) Correlation between P_PET
(h) Seasonality P
(i) Seasonality PET
(j) Slope
(k) Snowfall fraction
(l) Urbanized fraction
Percentage of significant trends (%)
5
4
3
2
L
M
H
Range